Haxhiu, Arber; Chan, Ricky; Kanerva, Sami; Kyyrä, Jorma

A system level approach to estimate maximum load steps that can be applied on a fuel cell powered marine DC system

Published in:
Energy Reports

DOI:
10.1016/j.egyr.2021.01.044

Published: 01/11/2021

Document Version
Publisher's PDF, also known as Version of record

Energy Reports 7 (2021) 888–895

Contents lists available at ScienceDirect

Energy Reports

journal homepage: www.elsevier.com/locate/egyr

A system level approach to estimate maximum load steps that can be applied on a fuel cell powered marine DC system

Arber Haxhiu [a,*], Ricky Chan [a], Sami Kanerva [a], Jorma Kyyrä [b]

[a] Electric Solutions, ABB Marine and Ports, Helsinki, Finland
[b] Electrical Engineering and Automation, Aalto University, Espoo, Finland

ARTICLE INFO

Article history:
Received 24 March 2020
Received in revised form 31 July 2020
Accepted 23 January 2021
Available online xxxx

Keywords:
Fuel cell model
System performance
Dynamic response
Marine power system
Modeling
PEM fuel cell

ABSTRACT

This paper presents a system level approach to estimate the maximum load steps on a hydrogen fuel cell powered marine system. In the proposed approach, a model has been developed to predict the system distribution voltage drop due to sudden load changes applied on the system. The estimated voltage drop is used as a metric to determine if a system can sustain the applied load change. Such technique is beneficial for system engineers in the early stage of marine system design and dimensioning. Additionally, the model can be used by a power management system to coordinate starting and stopping of fuel cells for improved system performance. In this work, the proposed approach is validated using a real-time hardware-in-loop simulation platform and it is demonstrated that the proposed approach is accurate within 1.2%.

1. Introduction

The maritime industry relies heavily on different fossil fuels for onboard propulsion and hotel energy. Burning fossil fuels for energy production releases large amounts of greenhouse gas (GHG) emissions, which is harmful for the environment. During 2012, the maritime industry accounted for approximately 2.8% of global GHG emissions (Smith et al., 2014). The International Maritime Organization (IMO) predicts that without any intervention, the GHG emissions from shipping will increase by up to 250% between 2012 and 2050. In order to avoid the rapid growth in GHG emissions, IMO has taken a decision to halve the total GHG emissions from the shipping industry by 2050. With the growing number of new vessels entering operation, the only way to achieve goals set by IMO is to replace high-emitting vessel power sources (i.e., diesel engines) with low or non-emitting alternatives.

For maritime applications, a promising alternative power source is the proton exchange membrane (PEM) fuel cell, as it offers green sustainable power production for marine vessels (Anon, 2018). Fuel cells are quiet power sources and have good energy efficiency at partial loads. However, the development of fuel cells as main power sources for marine vessels is still in its infancy. Utilizing fuel cells as main power sources for vessels require more performance and reliability analysis.

A PEM fuel cell produces electric current by combining hydrogen and oxygen in an electrochemical reaction. From this process, only heat and water are produced as byproducts. However, the dynamic characteristics of fuel cells differ significantly from more conventional marine power sources, such as diesel engines. Although fuel cells offer quick power ramp rates and high electrical efficiencies, they are very vulnerable to step load dynamics or fast transients where momentary load current exceeds the rate of reactant supply to the fuel cell (Nikiforow et al., 2018). Unlike diesel generators, fuel cells contain no inertial energy that can, to a certain extent, prevent the power supply from collapsing during a quick power steps or fast load power transients. This phenomenon, where the rate of extracted current exceeds the rate of fuel (hydrogen or oxygen) supply is typically referred to in the industry as fuel starvation. Starving the fuel cell from fuel, even for short periods, can significantly damage the fuel cells and cause a breakdown that would lead to a blackout (Pukrushpan et al., 2004; He et al., 2017). Like in most applications (e.g., electric vehicles), the aforementioned presents a challenge for marine vessels as well.

In the past decade, numerous dynamic fuel cell models have been developed in order to analyze and improve the dynamic response of PEM fuel cells. In particular, dynamic response of fuel cells during sudden load changes has been of interest. For example, a dynamic PEM fuel cell model based on flux balance concept (Chen et al., 2018b) was used to analyze how low fuel cell voltage drops and subsequently recovers following a sudden load transient. It is concluded that large rate of changes in current

* Corresponding author.
E-mail addresses: arber.haxhiu@fi.abb.com (A. Haxhiu), ricky.chan@fi.abb.com (R. Chan), sami.kanerva@fi.abb.com (S. Kanerva), jorma.kyyra@aalto.fi (J. Kyyrä).

https://doi.org/10.1016/j.egyr.2021.01.044

density lead to significant voltage drops and reduced operating efficiency. In Chen et al. (2018a), the impacts of operating temperature and pressure on fuel cell performance were investigated. Both are considered critical for finding optimal operation performance. In Edwards and Demuren (2016), a mathematical equation with multiple exponential terms was fitted to experimentally measured voltage data from single cells. The model was used to measure voltage dips following sudden load changes at fuel cell terminals. The membrane humidity level was shown to have a significant impact on the voltage dips following the transient. More system-oriented approaches were presented in Rabbani and Rokni (2013) and Hosseinzadeh and Rokni (2013) where dynamic models were developed for a 22.1 kW fuel cell stack, including common balance of plant (BOP) components, i.e., hydrogen feed system, air compressor, humidifier, thermal management system and control system. Sudden load changes were applied to the models and the voltage behavior was studied. It was demonstrated that increasing operating temperature and pressure improves fuel cell voltage dynamics, but it was also shown to be insufficient to prevent significant voltage drops following a sudden load transient. To improve fuel cell efficiency and electrical output power via operating parameter optimization, a multi-objective evolutionary algorithm based on decomposition was proposed in Chen et al. (2017). There it was shown that by optimization of operating parameters, the steady state performance of fuel cells can be improved. However, the challenge of inadequate fuel cell response to sudden load changes remains.

In light of the foregoing and other existing research on fuel cell power dynamics (San Martin et al., 2014; Corbo et al., 2009; Espiari and Aleyaasin, 2010; Padhee et al., 2015; Lee et al., 2010; Adzakpa et al., 2008), the fuel cell response to rapid load changes can be generalized as follows. The electrochemical reaction occurring on a cell level is very fast and allows for quick power response. On a system level (i.e., including BOP components), control of the critical operation processes is slow, thus lowering overall fuel cell power response. Due to the weak overall power response, it is commonly claimed that fuel cells cannot be used as sole power sources in marine vessels. Therefore, most research focuses on development of hybrid power systems with energy storage devices (e.g., batteries) used for enhanced dynamic performance (Shih et al., 2014; Díaz-de-Baldasano et al., 2014; Vafamand et al., 2020). However, proper studies on the dynamic response of a complete fuel cell powered system (e.g., a marine power system) are missing.

In marine applications, fuel cell power is generally controlled by power converters with quick power responses. The converters can prevent fuel cells from experiencing sudden load transients by controlling the fuel cell current according to fuel cell requirements (Na et al., 2007; Ziaeinejad et al., 2016; Amin et al., 2014). Therefore, the previous researches on dynamic response of single fuel cells cannot be referred directly to draw conclusions on the response of a complete system (powered only by fuel cells) to sudden load changes. Other factors such as load types, system voltage and energy stored in passive components must also be considered. Such a complex and interdependent system poses a challenge to system designers to determine the maximum load changes that can be applied on a purely fuel cell powered system without compromising on system reliability.

The work performed in this paper expands the existing research on fuel cell dynamics by studying how a purely fuel cell powered system responds to sudden load changes. The paper proposes an easily applicable system level approach using a closed form mathematical model to determine maximum load steps that can be applied on a purely fuel cell powered marine system. The emphasis is on systems with DC distribution due to their advantages compared to AC distribution systems for fuel cell integration to marine vessels. Similar to previous researches where the magnitude of fuel cell voltage drop following a power transient is used as a metric for dynamic response, this work uses the magnitude of the DC bus voltage drop as a metric for system dynamic response. The proposed approach is validated using a real-time hardware-in-loop (HIL) simulation setup consisting of previously validated power component models and actual power converter control units which are commercially available.

The proposed model is significant for both early stage system design and system control during operation. In early stage design of a marine power system, the model can be used to determine if a designed system can meet all operational load requirements. Such information is useful when deciding whether a system requires additional energy storage devices or can be powered purely by fuel cells. Regarding system control during operation, the model can be used by a shipboard power management system (PMS) to coordinate starting and stopping of fuel cells according to system load dynamics requirements. By estimating maximum allowed load steps in real-time, the PMS can pre-start fuel cells, e.g., prior to connection of large power consumers. When quick dynamics are not needed, the number of running fuel cells can decreased. The proposed approach is innovative because it considers a complete fuel cell powered system, instead of only a single fuel cell unit. System level studies on fuel cell powered systems are important in order to accelerate the adoption of fuel cells into marine vessels, and consequently reduce emissions from the shipping industry.

This paper is organized as follows. Section 2.1 provides a short introduction on PEM fuel cells and a commonly used fuel cell voltage model. The proposed approach is set forth in Section 2.2. Section 3 describes real-time HIL setup which is used to validate the proposed approach. The results of the HIL validation work are presented in Section 4. Additionally, Section 4 will show how different system variables affect the system response to sudden load changes. Finally, Section 5 concludes the work.

2. Estimation of DC bus voltage as a function of transient load power

2.1. Voltage characteristics of a PEM fuel cell

The PEM fuel cells are characterized by a low operating temperature (30–80 °C) and a solid electrolyte material. In its simplicity, a fuel cell consists of two catalyzed electrodes wrapped around a highly ion conductive electrolyte. A single fuel cell has an operating voltage between around 0.6 V to approximately 1.1 V. To obtain higher voltages, several fuel cells are connected in series to form fuel cell stacks. However, to be able to operate the fuel cell stack, several fuel cell subsystems, such as electronic controllers, a hydrogen delivery system, an oxygen (or air) delivery system, a cooling system and condition monitoring devices, are needed.

In order to estimate the behavior of a fuel cell powered system during a sudden load change, it is important to understand the voltage characteristics of the fuel cell. In the literature, numerous models have been proposed for estimation of fuel cell voltage as a function of current. One commonly used model is an empirical fuel cell model described in O'Hayre et al. (2016) and Larminie and Dicks (2003). The model thermodynamically estimates the fuel cell voltage at no load. As the fuel cell load increases, different voltage losses, i.e., losses due to reaction kinetics, charge transport and mass transport, are subtracted from the estimated no-load voltage. The model describes the fuel cell voltage as follows:

$$E_{fc} = N\left(E_{ocv} - A_a \ln\left(\frac{i_{fc}}{i_0}\right) - R_c i_{fc} - m_c e^{n_c i_{fc}}\right), \tag{1}$$

Table 1
Fuel cell model parameters used in the HIL tests of this work Haxhiu et al. (2019).

Parameter	Symbol	Value
Fuel cell open circuit voltage	E_{ocv}	1.1 V
Activation voltage drop coefficient	A_a	0.0525 V
Fuel cell exchange current	i_0	3.33 A
ion and electron transport resistivity	R_c	366 μΩ
Mass transport loss constant 1	m_c	0.77 μV
Mass transport loss constant 2	n_c	33.3 mA^{-1}

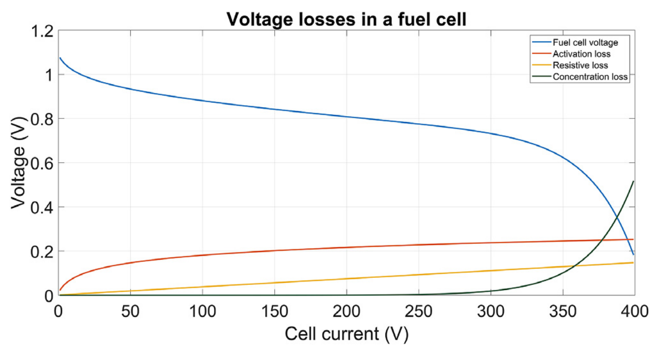

Fig. 1. The total fuel cell voltage and different fuel cell losses as function of current. Red, yellow and green lines represent fuel cell activation, resistive and mass transport voltage losses, respectively.. (For interpretation of the references to color in this figure legend, the reader is referred to the web version of this article.)

where, N is number of cells connected in series, E_{ocv} is no-load voltage, i_{fc} is fuel cell current, A_a is activation loss coefficient, i_0 is fuel cell exchange current, R_c is ion and electron transfer resistance and m_c and n_c are empirically determined constants. The second term $\left(E_{act} = A_a \ln\left(\frac{i_{fc}}{i_0}\right)\right)$on the right side of (1) describes the activation losses due to reaction kinetics. The third term ($E_{res} = R_c i_{fc}$), describes losses due ion and electron transport. Finally, the last term $\left(E_{con} = m_c e^{n_c i_{fc}}\right)$ describes the losses due to mass transport of reactants and products.

In practice, easiest way to obtain the parameters needed for (1) is by fitting the equation to a voltage polarization curve found in a datasheet from a fuel cell supplier. However, it should be noted that fuel cell voltage is highly dependent on fuel cell operating temperature and pressures. Therefore, if temperature or pressures are changed during operation, the parameters in (1) will be affected and would need to be redefined. However, in commercial fuel cell products for marine systems, temperature and pressures are normally pre-optimized by the product supplier. The supplier then provides a voltage curve as function of current. Therefore, in practice it would be enough to determine the parameters for (1) only once during the early system design phase. For this work, the parameters used in (1) are presented in Table 1. The total voltage and different voltage losses of a single cell obtained with (1) are illustrated in Fig. 1.

2.2. Derivation of the mathematical model to estimate system voltage dips during sudden load changes

In marine vessels with DC distribution, power sources and loads are centrally connected into a common DC bus through power converters as illustrated in Fig. 2. Each power converter is equipped with DC capacitors on the DC bus side. Due to short distances on board the vessel, impedance values from cables and busbars between the converters are commonly insignificant compared to the total amount of capacitance in the DC bus capacitors. Therefore, the DC bus can be modeled as a single large capacitor.

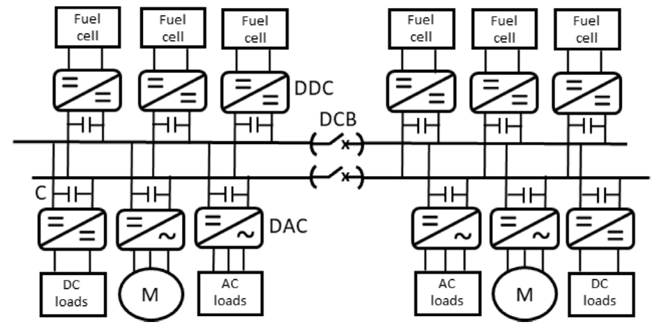

Fig. 2. A general fuel cell powered marine vessel power system with DC distribution. In the figure, DCB = DC breaker, DAC = DC/AC converter, DDC = DC/DC converter, C = capacitors and M = propulsion motor.

During operation, the DC bus voltage is kept constant by voltage-controlled power sources, e.g., a fuel cell with a DC/DC converter, connected on the DC bus. In order to regulate a steady DC bus voltage, the power sources are required to possess fast dynamic power responses. Quick incremental load power changes cause voltage dips which may lead to partial or complete system blackouts.

The voltage dip during a load transient is dependent on the magnitude of the transient and on the energy stored in the DC bus capacitors prior to the transient. Therefore, the following equation can be written for the change in DC bus voltage as function of time:

$$C_{bus}\frac{du(t)}{dt} = \frac{\left(\sum_{j=1}^{J} p_{s,j}(t) - \sum_{m=1}^{M} p_{l,m}(t)\right)}{u(t)}, \tag{2}$$

where u is DC bus voltage, t is duration of the transient, J is total number of power sources connected on the DC bus, $p_{s,j}$ is instantaneous power of a source j, M is total number of loads connected on the DC bus and $p_{l,m}$ is instantaneous power of a load m. By rearranging (3) and integrating both sides of the equation, the following is obtained:

$$C_{bus}\int_{u_i}^{u_f} u(t)du\,(t) = \int_{t_i}^{t_f}\left(\sum_{j=1}^{J} p_{s,j}\,(t) - \sum_{m=1}^{M} p_{l,m}\,(t)\right)dt. \tag{3}$$

Subscripts i and f are used to indicate initial and final values, respectively. Solving right side of (3) requires knowledge on the duration of the transient event (i.e., $\Delta t = t_f - t_i$) and supply and load powers of power sources and loads. The estimation of these variables is shown in the following section.

Observing (2), it can be noticed that change in voltage occurs only when there is imbalance between power production and consumption. During a sudden load increase, DC bus voltage keeps falling until power production meets power demand. Therefore, once duration Δt has passed since the first occurrence of the power transient, the changes in average power production and power consumption at the DC bus are equal and the following equation can be written:

$$\sum_{j=1}^{J}\Delta p_{s,j} - \sum_{m=1}^{M}\Delta p_{l,m} = 0, \tag{4}$$

where $\Delta p_{s,j}$ is power change in source j and $\Delta p_{l,m}$ is power change in load m. Since the transients usually occur randomly in the system, the approach herein assumes a worst-case scenario where the load powers increase instantly to their maximum value and stay there during the whole observation time. The following equation can be written to describe the change in total load power:

$$\Delta P_L = \sum_{m=1}^{M} \Delta p_{l,m}. \quad (5)$$

Inserting (5) into (4) and rearranging it yields

$$\sum_{j=1}^{J} \Delta p_{s,j} = \Delta P_L. \quad (6)$$

Recall that only fuel cell power sources are considered in this work. Therefore, $\Delta p_{s,j}$ in (6) can be replaced by Eq. (1) multiplied by fuel cell current as follows:

$$\sum_{j=1}^{J} E_{fc,j} i_j = \Delta P_L, \quad (7)$$

where $E_{fc,j}$ and i_j are voltage and current of fuel cell j, respectively.

Recalling from Section 1, fuel cell current must always be increased and decreased with a certain ramp rate, r_c, according to the fuel cell requirements. In practice, this ramp rate is typically limited by the response of an oxygen supply system (a controlled air compressor) (Nikiforow et al., 2018). Following a sudden load change, the fuel cell current is naturally increased until power production equals load consumption for duration Δt. Therefore, the following equation can be written for the fuel cell current:

$$i_j = i_{i,j} + r_{c,j} \Delta t, \quad (8)$$

where $i_{i,j}$ is the fuel cell current at the first instant when the load change occurs. Since fuel cell voltage $E_{fc,j}$ is a function of fuel cell current i_j and (8) shows fuel cell current to be a function of Δt, $E_{fc,j}$ is also a function of Δt. Therefore, by inserting (1) and (8) into (7), the duration Δt can be solved as a function of ΔP_L. However, since fuel cell voltage equation is a non-linear function of fuel cell current, it is more convenient to use a simpler approximation of the fuel cell voltage to solve Δt.

Earlier in Fig. 1, the fuel cell voltage was shown to decrease as a function of power due to activation, resistive and mass transport losses. The voltage losses due to mass transport become significant only at high current values (above ∼300 A in fuel cell of Fig. 1). Normally, it is not desirable to operate at such current levels because fuel cell efficiency is drastically decreased. Therefore, in this formulation, mass transport losses can be assumed negligible. On the other hand, activation voltage losses increase most significantly at low current values (<50 A in Fig. 1) and then the trend become almost linear. Therefore, it is appropriate to approximate activation losses about a current value near the fuel cell operating point by using first order Taylor polynomial (Adams, 2006):

$$E_{act,j} = N_j \left(A_{a,j} \left(\ln \left(\frac{a_j}{i_{0,j}} \right) - 1 \right) + \frac{A_j}{a_j} i_j \right), \quad (9)$$

where current a_j is the value about which the activation voltage drop of source j is approximated. Inserting (9) into (1) gives the following equation for the fuel cell voltage:

$$E_{fc,j} = N_j \left(E_{ocv,j} - A_{a,j} \left(\ln \left(\frac{a_j}{i_{0,j}} \right) - 1 \right) - \left(\frac{A_j}{a_j} + R_{c,j} \right) i_j \right). \quad (10)$$

Following the derivation of the approximated fuel cell voltage, the total power of all connected fuel cell power sources is obtained by inserting (8) into (10) and multiplying the result by (8). The total power of the fuel cell power sources at the instant Δt is given by the following equation:

$$\sum_{j=1}^{J} P_{fc,j}(\Delta t) = B\Delta t^2 + C\Delta t + D, \quad (11)$$

where

$$B = \sum_{j=1}^{J} -\left(\frac{A_{a,j}}{a_j} + R_{c,j} \right) r_{c,j}^2,$$

$$C = \sum_{j=1}^{J} N_c \left(E_{ocv,j} - A_{a,j} \left(\ln \left(\frac{a_j}{i_{0,j}} \right) - 1 \right) - 2 \left(\frac{A_{a,j}}{a_j} + R_{c,j} \right) i_{i,j} \right) r_{c,j}$$

and

$$D = \sum_{j=1}^{J} N_c \left(E_{ocv,j} - A_{a,j} \left(\ln \left(\frac{a_j}{i_{0,j}} \right) - 1 \right) - \left(\frac{A_{a,j}}{a_j} + R_{c,j} \right) i_{i,j} \right) i_{i,j}$$

are constants that can be derived using fuel cell model parameters.

The total power change in fuel cell sources can now be calculated as follows by subtracting the initial fuel cell powers i.e., power prior to the occurrence of the load transient from (11):

$$\sum_{j=1}^{J} \Delta p_{s,j} = \sum_{j=1}^{J} P_{fc,j}(\Delta t) - P_{init}, \quad (12)$$

where P_{init} is the total initial power of all connected fuel cell power sources. By further inserting (12) into (6), the following second order equation is obtained:

$$B\Delta t^2 + C\Delta t + D - P_{init} = \Delta P_L. \quad (13)$$

Eq. (13) has two solutions for Δt but only the closest positive solution from zero is applicable because that represents the first instance when power supply meets demand after the transient. Therefore, the solution to Δt is obtained from the following equation:

$$\Delta t = \frac{-C + \sqrt{C^2 - 4B(D - P_{init} - \Delta P_L)}}{2B}. \quad (14)$$

With the Δt solved, it is now possible to solve (3). This is achieved by first substituting (5) and (12) into (3) and then solving the integrals of both sides of (3). Hence, the following equation is obtained.

$$\frac{1}{2}\left(u_f^2 - u_i^2\right) = \frac{\frac{B\Delta t^3}{3} + \frac{C\Delta t^2}{2} + (D - P_{init} - \Delta P_L)\Delta t}{C_{cap}}. \quad (15)$$

Solving u_f from (15) gives the following equation for the DC bus voltage:

$$u_f = \sqrt{2\frac{\frac{B\Delta t^2}{3} + \frac{C\Delta t}{2} + [D - P_{init} - \Delta P_L]\,\Delta t}{C_{cap}} + u_i^2}. \quad (16)$$

The u_f is the lowest voltage level which is reached by the DC bus voltage following a sudden load change. It should be noted that during the derivation of (16) it was assumed that the load increase during the sudden load change occurs instantly. Often, however, load power is not expected to increase instantly but with a certain rise time, τ_L. In these cases, the final value where the DC bus voltage dips is obtained as follows:

$$u_f = \sqrt{2\frac{\frac{B\Delta t^2}{3} + \frac{C\Delta t}{2} + \left[D - P_{init} - \left(1 - \frac{\tau_L}{2}\right)\Delta P_L\right]\Delta t}{C_{cap}} + u_i^2}. \quad (17)$$

Eqs.(17) describes how a fuel cell powered system responds to sudden load changes by expressing how low the DC bus voltage dips due to the load change. Naturally, the accuracy of this mathematical model is highly dependent on the accuracy of the used fuel cell model. The validation of the model using the HIL test setup is presented in the next section.

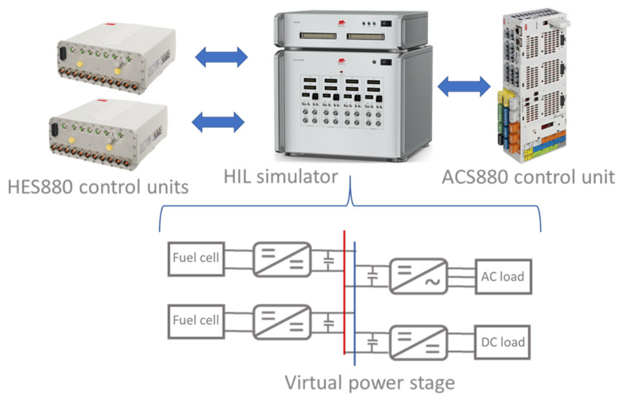

Fig. 3. The HIL test setup.

Table 2
Parameters used in the HIL fuel cell model.

Parameter	Symbol	Value
Fuel cell cathode double layer capacitance	C_{dl}	2.2 F
Oxygen activation energy at electrode	E_c	20 kj/mol
Electrochemical reaction symmetry factor	α	0.3709
Empirical parameter beta	β_c	3.32
Empirical parameter gamma	γ_C	1.1 A/m^2
Gas diffusion coefficient (O_2, H_2O)	$D_{O_2\_H_2O}$	30 μm^2/s
Gas diffusion coefficient (H_2, H_2O)	$D_{H_2\_H_2O}$	150 μm^2/s
Gas diffusion layer porosity	ε	35%
Gas diffusion layer tortuosity	τ	3
Membrane surface area	A_s	300 cm^2
Gas diffusion layer thickness	t_{gdl}	250 μm
Membrane thickness	t_m	112 μm
Hydrogen pressure at the anode	p_{h2}	2 Bar
Oxygen pressure at the cathode	p_{O2}	4 Bar
Temperature	T	334 K
Membrane water content	λ_{mem}	13
Number of cells	N	650
Weight per stack	m	65.45 g
Thermal capacity	c_p	879 J/(kg K)
Heat transfer coefficient	h_A	30 W/K
Reaction's enthalpy change	Δh	242 kJ/mol

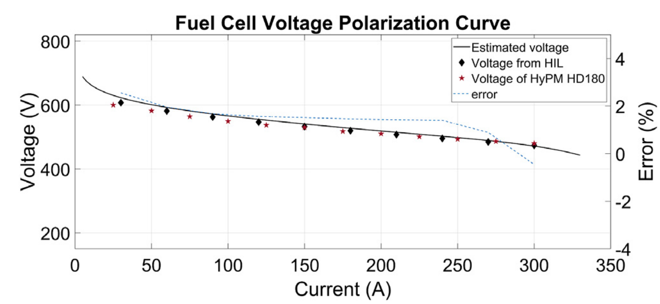

Fig. 4. Fuel cell voltage polarization curves. The dashed blue line presents the error (in percent) between the estimated voltage and voltage from the HIL model.. (For interpretation of the references to color in this figure legend, the reader is referred to the web version of this article.)

3. Description of the real time test setup

In order to test and validate the proposed approach for estimating the response of a fuel cell powered system, a real-time HIL setup was built. The HIL setup consists of a HIL simulator, two HES880 DC/DC converter control units and one ACS880 DC/AC converter control unit (ABB Oy, 2020a,b). The simulator operates with a 1 μs simulation step. The two three control units are connected to the HIL simulator through hardwired high-speed input and output terminals. A virtual power stage consisting of two fuel cells with DC/DC converters, one AC load with a DC/AC inverter and one DC load with a DC/DC converter was modeled. The HES880 control units are used to control the virtual power stages of fuel cell DC/DC converters and the ACS880 control unit is used to control the virtual power stage of the DC/AC converter. The test setup is illustrated in Fig. 3. The DC load DC/DC converter was controlled with a pulse width modulation (PWM) control method using a signal processing toolbox from Typhoon HIL (Typhoon HIL, 2018a). Each capacitor in the DC bus has a 15 mF capacitance.

The fuel cells in the HIL setup are modeled using pre-validated fuel cell models in the Typhoon HIL library (Typhoon HIL, 2018b). The nominal power of the fuel cell is 150 kW. The models consider the electrochemical, the fluidic and the thermal processes in a fuel cell. All parameters required by the fuel cell model are presented in Table 2. For comparison, the fuel cell voltage polarization curve obtained with (1) and parameters from Table 1 is compared to that obtained from the HIL system. The comparison is presented in Fig. 4. For reference, the voltage polarization curve of HyPM HD180 from Hydrogenics is also included in the figure (HYDROGENICS Corporation, 2012). It is included to show that the HIL simulated and estimated voltages are in accordance with those of a real commercial fuel cell product suitable for marine applications (Pratt and Klebanoff, 2016). The blue dashed lines in Fig. 4 show that the accuracy between the estimated voltage and the voltage from the HIL model is within 2%. Therefore, the empirically obtained parameters in (1) are considered sufficiently accurate to estimate the system response with the approach proposed in this work.

4. Results and discussion

4.1. HIL results in time domain

In order to validate the accuracy of the proposed approach, two separate tests were performed in the HIL setup. In these tests, the fuel cell powered system was initially operated in steady state and then three sudden load changes with different magnitudes were applied on the system. Each load change was applied approximately two seconds after the DC voltage recovered to its nominal value of 750 V in these tests. Each fuel cell is controlled with a maximum increasing current ramp rate of 20 A/s. The minimum allowed DC bus voltage is 600 V. If the DC bus voltage drops below 600 V, the system is considered not be able to endure the load transient and it will trigger additional system protection responses. The tests were performed to see how accurately the magnitude of the voltage drop can be estimated using (17).

In the first test, only one fuel cell was operated and the other was off. The fuel cell initially supplied 12.5 kW to an AC load and 33 kW to a DC load. The sudden load changes were applied on the system as follows. At 0.5 s, the DC load was increased by 6.67 kW. At 3 s, the DC load was further increased by 10 kW. Finally, at 7 s, the DC load was increased by an additional 12.5 kW. In each load step, the rise time τ_L of the load increase was 250 ms. The impacts of the load transients on the DC bus voltage are illustrated in Fig. 5. The blue line in the figure illustrates the behavior of the DC bus voltage. The red, green and yellow lines illustrate the behavior of fuel cell power, DC load power and AC load power, respectively. The black diamonds are the estimated DC bus voltage drop as described by (17).

Due to the slowness in the fuel cell power adjustment, the DC bus voltage dips significantly after each load change. The impact from the first and the second load change is estimated with a good accuracy and within 1.2%. However, in the third load step, the DC bus voltage is estimated to drop to ∼570 V but in the

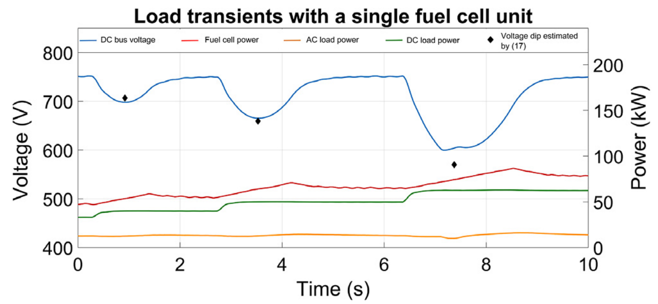

Fig. 5. HIL simulated voltage dips with three different power transient steps (6.67 kW at 0.5 s, 10 kW at 3 s and 12.5 kW at 7 s). Only one fuel cell is powering the loads.

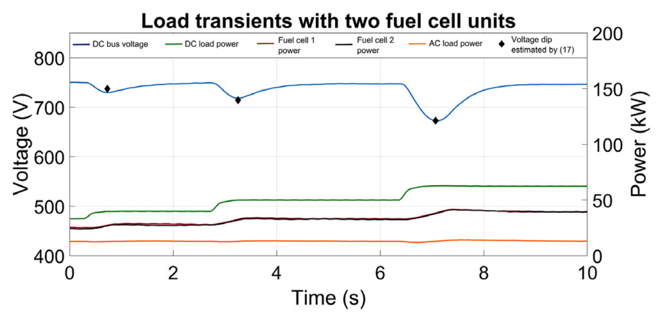

Fig. 6. HIL simulated voltage dips with three different power transient steps (6.67 kW at 0.5 s, 10 kW at 3 s and 12.5 kW at 7 s). Two fuel cells are powering two loads (AC load and DC load)

HIL setup it drops only to ~600V. The reason for the Smaller voltage drop is the activation of undervoltage control function in the DC/AC converter. Once DC/AC voltage reaches 600 V, the DC/AC converter immediately reduces its load, and thus the 600 V DC voltage is maintained. The load reduction can be seen as a small dip in AC power in Fig. 5. Without the activation of undervoltage control, the DC voltage would have dropped closer to the estimated 570 V. Nevertheless, it is evident that the last load change interrupted reliable load supply.

In the second test of this work, both fuel cell in the HIL setup were operated. Same load power changes as in the first test were applied on the fuel cell powered system. To ensure equal load sharing between the two fuel cells, the DC/DC converters are operated with a 5% DC voltage droop control. The impacts of the load transients on the DC bus voltage are illustrated in Fig. 6. In accordance with the first test, the error between estimated voltage drop and the voltage drop in the HIL setup is less than 1.2%. This time, none of loads were large enough to cause instability in the system.

By comparing the results of the first and second test, it can be seen that when the system is powered by one fuel cell only, the system is able to sustain a 10 kW load change without interruption to load supply. However, a 12.5 kW load change resulted in power limitation by the DC/AC converter. The same did not occur in the second test because two fuel cells were supplying power, instead of one. In a marine vessel, it is important that enough fuel cells are powering the system so that critical load supply is never interrupted. The starting and stopping of power sources is typically handled by a shipboard PMS. The information provided by (17) is important to the PMS because it could prevent start-up of heavy loads until enough fuel cells are connected and supplying power. That way, the system is kept robust.

The numeric values of results from the HIL tests are presented in Table 3. The maximum increasing fuel cell current ramp rate was set to 20 A/s but during the tests, it was observed that the actual ramp rate varied between 17 A/s to 21 A/s. In both test cases, the error between HIL simulated values and the estimated values (excluding third load transient of test one) was less than 1.2% of nominal DC bus voltage. Therefore, the accuracy of the model proposed in this work is considered commendable.

Table 3
Comparison of HIL simulated results to estimated results. Error column indicates the difference between HIL simulated value and estimated value as a percentage of nominal DC bus voltage (750 V in this work).

Test	Load change	u_f (HIL test)	u_f (estimate)	r_c	Error
1	6,67 kW	697.9 V	706.7 V	18 A/s	1.20%
	10.0 kW	665.2 V	659.4 V	21 A/s	0.80%
	12.5 kW	599.6 V	569.9 V	19 A/s	N/A
2	6,67 kW	723.8 V	731.7 V	19 A/s	1.10%
	10.0 kW	711.6 V	706.8 V	20 A/s	0.60%
	12.5 kW	664.5 V	664.8V	17 A/s	0.00%

4.2. Parameters determining the magnitude of the voltage drop

The two tests performed in this work show that if 600 V is chosen as minimum allowed DC bus voltage, the maximum power transient that a single fuel cell (with parameters used in this work) can endure is around 7.5% of nominal power of the fuel cells. However, by observing the derivation of Eq. (17), it can be noticed that there exist several variables that can be used to improve the maximum allowed load step. All other fuel cell parameters being constant, five variables determine how low the DC bus voltage will dip during a power transient on the DC bus. These factors are the magnitude of the load step (ΔP_L) compared to the available fuel cell power, DC bus voltage level prior to the transient (u_i), the amount of capacitance in the common DC bus (C_{cap}), the fuel cell current prior to the transient (i_i) and the maximum allowed fuel cell current ramp rate (r_c). The impacts of each of these variables on the DC bus voltage dip are illustrated in the following Figs. 7–10. The waveforms in the following figures are calculated considering only one fuel cell power source and the nominal DC bus voltage remains at 750 V. In each figure, the Y-axis shows the lowest point in the DC bus voltage dip after a load change has been applied. For reference, some of the operating points in the following figures are also verified using the HIL simulation setup presented earlier. In the figures, the HIL simulated values are illustrated using crosses while the values estimated with (17) are illustrated with solid lines.

Fig. 7 illustrates the impact of load change magnitude to the DC bus voltage drop. Three different (700 V, 750 V and 800 V) initial voltage levels are studied. Naturally, increasing load change causes larger voltage dips and the lower the initial DC voltage, the larger the voltage dip. Nevertheless, it is interesting to notice that a 50 V DC voltage increase can have a significant impact on improving the durability of the system to load changes. For example, if $u_i = 700$ V prior to a load change, a 9-kW load leads to DC bus voltage dropping to 600 V. However, if $u_i = 750$ V, a 12-kW load change is needed for the voltage to drop to 600 V. This represents 33% increase in system durability to load changes.

The impact of DC bus capacitance is shown in Fig. 8. The capacitors are energy storage devices and therefore, increasing the capacitance improves the system durability to load changes. However, as shown in the figure, after a certain point the improvement saturates. For optimal dimensioning, the capacitance value should be selected as low as possible to minimize the onboard footprint requirement, while still ensuring that the DC bus voltage does not exceed the minimum allowed voltage level during a power transient.

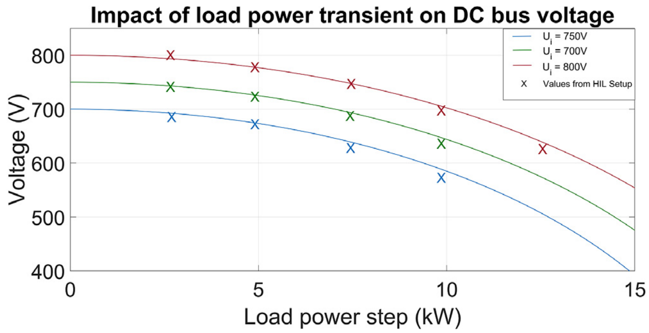

Fig. 7. A graphical illustration of how low the DC bus voltage dips due to a load power transient. The impact is illustrated with three different initial voltage levels. The solid lines are illustrations of how low the proposed method estimates the voltage to dip due to the transients, while the crosses are HIL simulated values.

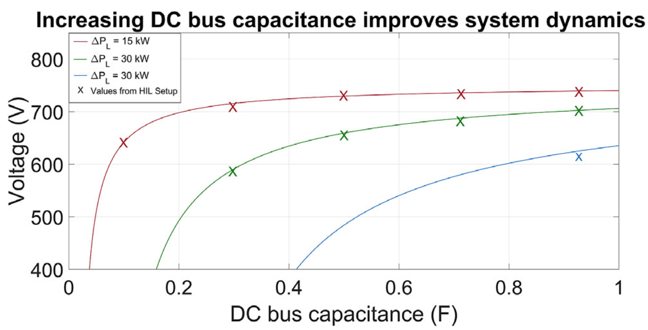

Fig. 8. Impact of the DC bus capacitance on how low the DC bus voltage dips (from nominal voltage 750 V) during a transient event. The impact is illustrated with three different magnitudes of transient power. The solid lines illustrate calculated voltage dips and the crosses illustrate respective HIL simulated results.

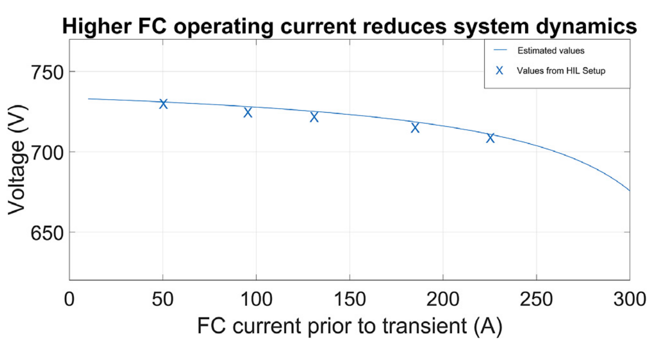

Fig. 9. Impact of the initial fuel cell current (pre transient event) on how low the DC bus voltage dips (from nominal voltage 750 V) during a power transient (5% of fuel cell nominal). The line illustrates calculated voltage dips and the crosses illustrate respective HIL simulated results.

Fig. 9 shows the impacts of the fuel cell operating point, i.e., fuel cell current level, to the magnitude of the DC bus voltage drop. As stated earlier, the fuel cell voltage is a non-linear function of fuel cell current. Due to the lower voltage at higher current, a power increase at higher operating points will require higher current increase compared to lower operating points. Therefore, at higher operating points, a sudden load change will result in a larger DC bus voltage dip. It is important to be aware of this phenomenon to ensure reliable operation over complete fuel cell operation range.

Finally, Fig. 10 illustrates the impacts of maximum allowed fuel cell current ramp rate on the DC voltage drop. Naturally, this parameter has a significant impact on the dynamic power

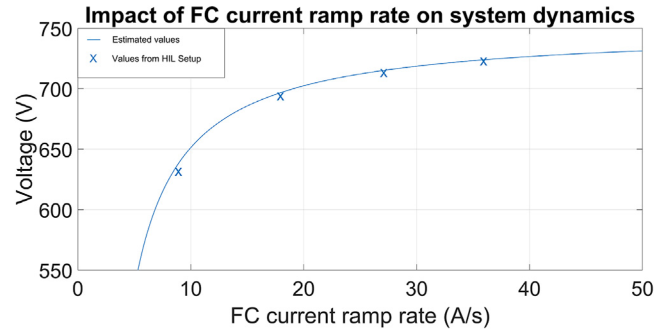

Fig. 10. Impact of fuel cell current ramp rate on how low the DC bus voltage dips (from nominal voltage 750 V) during a power transient (5% of fuel cell nominal). The line illustrates calculated voltage dips and the crosses illustrate respective HIL simulated results.

characteristics of a fuel cell. If the fuel cell current ramp rate is too low (e.g., less than ∼15 A/s in fuel cell of Fig. 10), the DC bus voltage collapses due to the system's inability to respond to the applied load change. However, even if the fuel cell current ramp rate is significantly increased, (e.g., from 30 A/s to 50 A/s in fuel cell of Fig. 10), after a certain point, the difference in DC bus voltage drop magnitude becomes insignificant. Earlier in this work, it was mentioned that in practice, fuel cell current ramp rate is usually limited by the response rate of its oxygen supply subsystem (namely air compressor). If higher response rates are desired, a more powerful oxygen supply subsystem is needed. Therefore, it is important to be aware of the tradeoff between the system response as required according to the operational profile and the subsystem's performance, complexity, and cost.

5. Conclusion

In conclusion, a mathematical model has been set forth in this work to estimate the maximum load steps that can be applied on purely fuel cell powered marine systems. The fidelity of the model was validated using a real-time HIL setup. The results demonstrate that the accuracy of the mathematical model is very commendable with the error between HIL and estimated results being within 1.2%. The small error between the results is expected due to approximations applied in the proposed estimation method and the overall mismatch between the used empiric voltage model and the measured HIL fuel cell voltage. In addition, this work illustrates the impacts of several system parameters to the system response so as to aid marine system engineers in analyzing the tradeoffs to optimize the design according to the requirements and vessel operational profile.

For future work, this approach can be applied in conjunction with a vessel PMS as, for example, conditions for load dependent start and stop functions or prevention of large consumer start-up.

CRediT authorship contribution statement

Arber Haxhiu: Conceptualization, Methodology, Validation. **Ricky Chan:** Conceptualization, Review. **Sami Kanerva:** Conceptualization, Review. **Jorma Kyyrä:** Supervision, Review.

Declaration of competing interest

The authors declare the following financial interests/personal relationships which may be considered as potential competing interests: The authors Arber Haxhiu, Sami Kanerva and Ricky chan are full-time employees at ABB Marine and Ports, while Jorma Kyyrä is a full-time professor in Aalto University, Finland.

References

ABB Oy, 2020a. HES880 Mobile Drive. [Online]. Available: https://new.abb.com/drives/low-voltage-ac/industry-specific-drives/hes880. (Accessed 23 March 2020).

ABB Oy, 2020b. ACS880-104 - inverter modules. [Online]. Available: https://new.abb.com/drives/low-voltage-ac/industrial-drives/acs880-drive-modules/acs880-104. (Accessed 23 March 2020).

Adams, R., 2006. Calculus: A Complete Course, sixth ed. Pearson Addison Wesleay, Toronto.

Adzakpa, K., Agbossou, K., DubÉ, Y., Dostie, M., Fournier, M., Poulin, A., 2008. PEM fuel cells modeling and analysis through current and voltage transient behaviors. IEEE Trans. Energy Convers. 23 (2), 581–591.

Amin, Bambang, R.T., Rohman, A.S., Dronkers, C.J., Ortega, R., Sasongko, A., 2014. Energy management of fuel cell/battery/supercapacitor hybrid power sources using model predictive control. IEEE Trans. Ind. Inf. 10, 1992–2002.

Anon, 2018. Assessment of Selected Alternative Fuels and Technologies. Det Norske Veritas and Germanischer Lloyd – Maritime.

Chen, B., Cai, Y., Shen, J., Tu, Z., Chan, S., 2018a. Performance degradation of a proton exchange membrane fuel cell with dead-ended cathode and anode. Appl. Therm. Eng. 132, 80–86.

Chen, H., Jia, S., Liu, B., Zhang, T., 2018b. Numerical simulation of the power performance a proton exchange membrane fuel cell under dynamic loading conditions. IEEE Access 6, 67992–68000.

Chen, X., Li, W., Gong, G., Wan, Z., Tu, Z., 2017. Parametric analysis and optimization of PEMFC system with maximum power and efficiency using MOEA/D. Appl. Therm. Eng. 121, 400–409.

Corbo, P., Migliardini, F., Veneri, O., 2009. Dynamic behaviour of hydrogen fuel cells for automotive application. Renew. Energy 34, 1955–1961.

Díaz-de-Baldasano, M., Mateos, F., Núñez Rivas, L., Leo, T., 2014. Conceptual design of offshore platform supply vessel based on hybrid diesel generator-fuel cell power plant. J. Appl. Energy 116, 91–100.

Edwards, R., Demuren, A., 2016. Regression analysis of PEM fuel cell transient response. Int. J. Energy Environ. Eng. 7, 329–341.

Espiari, S., Aleyaasin, M., 2010. Transient response of PEM fuel cells during sudden load change. In: 2010 IEEE International Energy Conference, Manama, pp. 211–216.

Haxhiu, A., Kyyrä, J., Chan, R., Kanerva, S., 2019. A variable DC approach to minimize drivetrain losses in FC marine power systems. In: IEEE Power and Energy Conference at Illinois, pp. 1–6.

He, L., Han, Z., Liu, Y., Niu, Z., Liu, Z., 2017. Effects of gas starvation on performance of a single PEMFC. In: IEEE Transportation Electrification Conference and Expo, Asia-Pacific.

Hosseinzadeh, E., Rokni, M., 2013. Development and validation of a simple analytical model of the proton exchange membrane fuel cell (pemfc) in a fork-lift truck power system. Int. J. Green Energy 10, 523–543.

HYDROGENICS Corporation, 2012. HyPM HD180 Datasheet, Heavy Duty Fuel Cell Power Module. [Online]. Available: https://pdf.directindustry.com/pdf/hydrogenics/hypm-hd-180/33492-420321.html. (Accessed 20 July 2020).

Larminie, J., Dicks, A., 2003. FC Systems Explained, second ed. John Wiley & Sons Ltd., Chichester.

Lee, Y., Choi, Y., Zhang, Y., Lee, K., 2010. Dynamic transient phenomena of a proton exchange membrane fuel cell. J. The Korean Inst. Electr. Electron. Mater. Eng. 23, 530–533.

Na, W.K., Gou, B., Diong, B., 2007. Nonlinear control of PEM fuel cells by exact linearization. IEEE Trans. Ind. Appl. 43 (6), 1426–1433.

Nikiforow, K., Pennanen, J., Ihonen, J., Uski, S., Koski, P., 2018. Power ramp rate capabilities of a 5kW proton exchange membrane FC system with discrete ejector control. J. Power Sources 381, 30–37.

O'Hayre, R., Cha, S., Colella, W., Prinz, F., 2016. FC Fundamentals, first ed. John Wiley & Sons Inc., Hoboken.

Padhee, S., Pati, U., Mahapatra, K., 2015. Investigation on transient response of fuel cell power conditioning unit during rapid load changes. In: 2015 IEEE International Conference on Computational Intelligence & Communication Technology, Ghaziabad, pp. 482–487.

Pratt, J.W., Klebanoff, L.E., 2016. Feasibility of the SF-BREEZE: A Zeroemission, Hydrogen FC, High-Speed Passenger Ferry. Sandia National Laboratories, Livermore, California.

Pukrushpan, J., Stefanopoulou, A., Peng, Huei, 2004. Control of FC breathing. IEEE Control Syst. Mag. 24, 30–46.

Rabbani, R., Rokni, M., 2013. Dynamic characteristics of an automotive fuel cell system for transitory load changes. Sustain. Energy Technol. Assess. 1, 34–43.

San Martin, I., Ursua, A., Sanchis, P., San Martin, I., Ursua, A., Sanchis, P., 2014. Modelling of PEM FC performance: Steady-state and dynamic experimental validation. Energies 7, 670–700.

Shih, N., Weng, B., Lee, J., Hsiao, Y., 2014. Development of a 20 kW generic hybrid fuel cell power system for small ships and underwater vehicles. Int. J. Hydrogen Energy 39, 13894–13901.

Smith, T., O'Keeffe, E., Aldous, L., Parker, S., Raucci, C., Traut, M., Corbett, J., Winebrake, J., Jalkanen, J., Johansson, L., Anderson, B., Agrawal, A., Ettinger, S., Ng, S., Hanayama, S., Faber, J., Nelissen, D., Hoen, M., Lee, D., Chesworth, S., Pandey, A., 2014. Third IMO GHG Study 2014. International Maritime Organization, London.

Typhoon HIL, 2018a. Typhoon HIL schematic library. [Online]. Available: https://www.typhoon-hil.com/documentation/typhoon-hil-schematic-editor-library/References/three-phase_two-level_inverter_rectifier.html?hl=inverter. (Accessed 23 March 23 2020).

Typhoon HIL, 2018b. Fuel Cell From Typhoon HIL schematic library. [Online]. Available: https://www.typhoon-hil.com/documentation/typhoon-hil-schematic-editor-library/References/fuel_cell.html. (Accessed 23 March 2020).

Vafamand, N., Boudjadar, J., Khooban, M., 2020. Model predictive energy management in hybrid ferry grids. Energy Rep. 6, 550–557.

Ziaeinejad, S., Sangsefidi, Y., Mehrizi-Sani, A., 2016. Fuel cell-based auxiliary power unit: EMS, sizing, and current estimator-based controller. IEEE Trans. Veh. Technol. 65 (6), 4826–4835.